

# Degradation Photoinduced by Fe(III): Method of Alkylphenol Ethoxylates Removal in Water

NATHALIE BRAND,  
GILLES MAILHOT, AND MICHÈLE BOLTE\*

Laboratoire de Photochimie Moléculaire et Macromoléculaire,  
Unité Mixte de Recherche CNRS-Université Blaise Pascal 6505,  
F-63177 Aubière Cedex, France

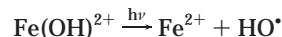
The photoinduced degradation of an alkylphenol ethoxylate (APE) (Igepal CA 520) by Fe(III) in aqueous solution has been investigated. A complete characterization of the commercial product showed the presence of a mixture of compounds with various ethoxy and alkyl chain lengths. The photodegradation study was carried out with the major fraction of ethoxymers having an alkyl chain length of 8 carbon atoms and  $n$  ethoxy units E ( $C_8PhE_n$ ). We have demonstrated that the Fe(III) sensitized degradation of this fraction occurs efficiently both at 365 nm and under sunlight. The rate of degradation depends on the concentration of  $Fe(OH)^{2+}$ , the most photoreactive species in terms of  $\cdot OH$  radical formation. The primary step of the decomposition of Igepal involves the hydrogen abstraction on one carbon of the ethoxy chain. The shortening of the ethoxylated chain all along the degradation process was observed. The identified photoproducts are aldehyde ethoxylates, formate ethoxylates, and octylphenol that is a persistent product in the environment. The mechanism only involves attack by  $\cdot OH$  radicals that are formed through photolysis of  $Fe(OH)^{2+}$ . For prolonged irradiations, the total degradation of Igepal CA 520 and of the photoproducts is obtained. Consequently, the degradation photoinduced by Fe(III) could be an efficient method of APEs removal in water.

## Introduction

Alkylphenol ethoxylates (APEs) have been used for more than 40 years as detergents, emulsifiers, and wetting and dispersing agents in household products and in agricultural and industrial applications. As a result, APEs are scattered in large amounts into the aquatic environment. Consequently, they have been and still are the focus of discussion on environmental acceptability (1). It was discovered in 1984 (2) that APEs were transformed into more toxic compounds during the biodegradation that accompanies wastewater treatment. The metabolites were also shown to be more persistent and more lipophilic than the parent APEs, leading to an additional problem of bioaccumulation. Since this discovery, the biodegradation of APEs has been extensively studied (3–6), but the pathway of ultimate biodegradation remains unproved. Several papers (7–9) deal with the photoinduced catalytic decomposition of APEs, particularly

the efficiency of the photocatalytic degradation of these compounds by using  $TiO_2$  particulates has been established and complete conversion to  $CO_2$  has been demonstrated (8). Consequently, the photodecomposition of APEs seems to be a promising route for the treatment of water.

In our laboratory, we have previously investigated the degradation of pollutants photoinduced by Fe(III) (10–12). Fe(III)–aquo complexes are known to undergo photolysis upon irradiation with wavelengths  $\lambda > 300$  nm, yielding Fe(II) and hydroxyl radicals ( $\cdot OH$ ) (13, 14). Among the Fe(III)–aquo complexes,  $Fe(OH)^{2+}$  is photolyzed with the highest quantum yield (13), according to the following reaction:



Hydroxyl radicals are known to be very reactive species, reacting with most organic substrates with rate constants that are limited by diffusion. In all cases, we concluded that the degradation photoinduced by Fe(III) was an interesting process for the elimination of pollutants in aqueous solution.

## Experimental Section

**Reagents and Solutions.** Igepal CA 520 and 4-(*tert*-octyl)-phenol (97%) were purchased from Aldrich and used without further purification. Ferric perchlorate nonahydrate [ $Fe(ClO_4)_3 \cdot 9H_2O$ ; 97%] and barium hydroxide octahydrate [ $Ba(OH)_2 \cdot 8H_2O$ ; puriss] were Fluka products kept in a desiccator. The Fe(III) solutions for the studies were prepared by diluting stock solutions [ $2.0 \times 10^{-3}$  mol  $L^{-1}$  in  $Fe(ClO_4)_3 \cdot 9H_2O$ ] to the appropriate Fe(III) concentration. The percentage in  $Fe(OH)^{2+}$ , the major monomeric species, was determined. Formic acid (80%) and 2-propanol (HPLC grade chromanorm > 99.7%) were Prolabo products. All solutions were prepared with deionized ultrapure water ( $\rho = 18.2$  M $\Omega$  cm). pH measurements were carried out with an ORION pH meter to 0.01 unit. The ionic strength was not controlled.

**Apparatus.** UV–vis spectra were recorded on a CARY 3 double beam spectrophotometer.

HPLC experiments were carried out using a Waters 540 chromatograph equipped with a Waters 996 photodiode array detector giving the UV–vis spectrum corresponding to each peak. The flow rate was 1 mL  $min^{-1}$ . Liquid chromatography/positive electrospray/mass spectra (LC/ES/MS) were obtained from “Service Central d’Analyse”, CNRS, Vernaison, France. The flow rate was 0.3 mL  $min^{-1}$ . In both cases, the eluent was a mixture of acetonitrile/water and the column was a Touzard and Matignon Kromasil  $C_{18}$  (250 mm long  $\times$  4.6 mm i.d., p.d. 5  $\mu m$ ).

$^1H$  NMR spectra were recorded on a BRUKER AC 400 MHz Fourier transform spectrometer.

To measure the quantum yields, the monochromatic irradiations at 296, 313, and 365 nm were carried out with a high-pressure mercury lamp (Osram HBO 200W) equipped with a grating monochromator (Bausch and Lomb). The beam was parallel and the reactor was a quartz cell of 1 cm path length. The light intensity was measured by ferrioxalate actinometry (15) [ $I_{(365nm)} \approx 3.7 \times 10^{15}$  photons  $s^{-1} cm^{-2}$ ;  $I_{(313nm)} \approx 2 \times 10^{15}$  photons  $s^{-1} cm^{-2}$ ;  $I_{(296nm)} \approx 9.8 \times 10^{14}$  photons  $s^{-1} cm^{-2}$ ].

A second irradiation setup used for kinetic experiments was an elliptical stainless steel cylinder. A high-pressure mercury lamp (Philips HPW type 125W), the emission of which at 365 nm was selected by an inner filter, was located at a focal axis of the elliptical cylinder. The reactor, a water-

\* Corresponding author phone: 33 (0)4 73 40 71 71; fax: 33 (0)4 73 40 77 00; e-mail: boltem@cicsun.univ-bpclermont.fr.

jacketed Pyrex tube (diameter = 2.8 cm), was centered at the other focal axis. The reaction medium was well stirred. The unit delivered an intensity  $I_0 \approx 4.6 \times 10^{15}$  photons  $s^{-1} cm^{-2}$  over a large volume (60 mL).

Solar irradiations were carried out into a Pyrex cylindrical reactor during summer-time in Clermont-Ferrand (latitude  $46^\circ N$ ; 400 m above sea level).

**Analysis.** The Fe(II) concentration was determined by complexometry with *o*-phenanthroline, using  $\epsilon_{510} = 1.118 \times 10^4 L mol^{-1} cm^{-1}$  for the Fe(II)–phenanthroline complex (15).

The method to measure the monomeric concentration of Fe(III) was modified from Küenzi's procedure (16). One milliliter of  $0.05 mol L^{-1}$  8-hydroxyquinoline-5-sulfonic acid (HQSA) and 1 mL of acetic buffer (pH 4.6) were poured into a 10 mL volumetric flask. Eight milliliters of sample was added to the solution and rapidly mixed. Within 30 s of mixing, the absorbance of the triscomplex of 8-hydroxyquinoline-5-sulfonate (HQS) with Fe(III),  $Fe(HQS)_3$ , was measured at  $\lambda = 572 nm$ . The same mixture of HQSA and acetic buffer with 8 mL of water was used as a blank. HQSA reacted much more rapidly with monomeric Fe(III) species than with either the Fe(III) dimer or Fe(III) polymers. The complex  $Fe(HQS)_3$  absorbed in a spectral region (572 nm) where neither the Fe(III) dimer nor the Fe(III) polymers/precipitates absorb. An  $\epsilon$  value of  $5070 \pm 100 mol L^{-1} cm^{-1}$  for  $Fe(HQS)_3$  at 572 nm deduced from the literature (13, 16) was used in this work.

Under our experimental conditions ( $c = 3.0 \times 10^{-4} mol L^{-1}$  and pH 3.50),  $Fe(OH)^{2+}$  [ $Fe(OH)^{2+}$  refers to  $Fe(OH)(H_2O)_5^{2+}$ ] is the predominant monomeric Fe(III) hydroxy complex (13). However, the concentration of monomeric species rapidly decreased after the dissolution of ferric perchlorate in water. The disappearance was attributed to the possible formation of aggregates, the first step toward the formation of soluble polymeric species and the precipitation of amorphous  $Fe(OH)_3$  (29). It appeared that the percentage of  $Fe(OH)^{2+}$  strongly depended on the age of the ferric solution and on the starting concentration (13). By the HQSA method (see Experimental Section), we were able to determine the percentage of  $Fe(OH)^{2+}$  in solution:

$$\%Fe(OH)^{2+} = \frac{[Fe(OH)^{2+}]}{[Fe(III)]_{to}} \times 100$$

$[Fe(III)]_{to}$  is the concentration of total dissolved Fe(III). The different percentage of  $Fe(OH)^{2+}$  was obtained by the use of Fe(III) solutions of different age. The  $\sim 100\%$  of  $Fe(OH)^{2+}$  was obtained by weighing the desired amount of  $Fe(ClO_4)_3$  and by using the resulting solution immediately after the dissolution.

Igepal CA 520 ( $c = 4.6 \times 10^{-4} mol L^{-1}$ ) degradation and photoproducts formation were followed by HPLC (UV detection at 226 nm) by measuring the areas of the corresponding peaks.

Carbon dioxide produced upon irradiation was determined as  $BaCO_3$ . It was removed from the solutions by an oxygen flow [scrubbed from  $CO_2$  traces by passing through a concentrated  $Ba(OH)_2$  solution] and trapped in two consecutive  $6.0 \times 10^{-3} mol L^{-1}$   $Ba(OH)_2$  solutions. The solutions were collected,  $BaCO_3$  allowed to precipitate and the excess of  $Ba(OH)_2$  was titrated with a  $6.0 \times 10^{-3} mol L^{-1}$  HCl solution. A blank experiment was performed under the same conditions but without Igepal CA 520.

## Results and Discussion

**Characterization of Igepal CA 520.** Igepals are prepared by the reaction of ethylene oxide with alkylphenols in the

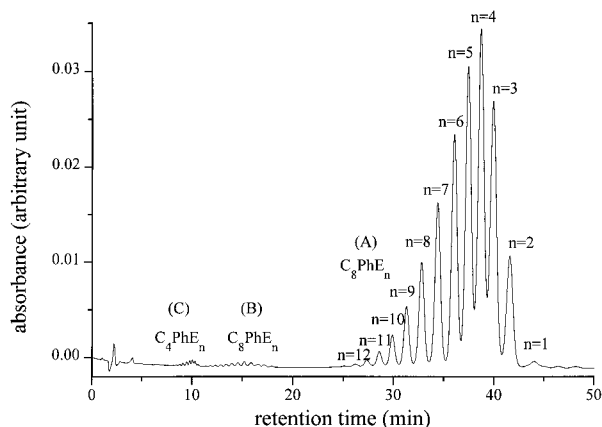
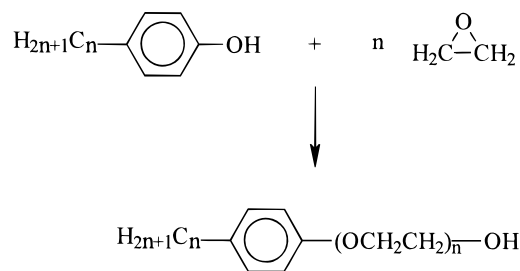


FIGURE 1. HPLC chromatogram of an aqueous solution of Igepal CA 520 ( $4.6 \times 10^{-4} mol L^{-1}$ ). Detection:  $\lambda = 226 nm$ . Eluent: acetonitrile + water (55/45 v/v).

presence of catalysts to give molecules where the hydrophobic part consists of alkylphenols:



However, this reaction is not as precisely controlled as the equation would indicate. Consequently, commercial products contain a mixture of various polyoxyethylene chain lengths as well as free polyoxyethylene glycol and unreacted matter (17).

Igepal CA 520 is manufactured as an octylphenol polyethoxylate ( $C_8\text{PhE}_n$ ) with an average number of ethylene oxide units  $n$  equal to 5. Analysis of APEs have been the subject of many papers or books in the last 20 years (17–19). Liquid chromatography appears to be the most suitable technique for the quantitative analysis of APEs: normal-phase chromatography allows to separate the ethoxymers only (20–23); reversed-phase chromatography resolved the alkyl chains but not permitted to separate the ethoxymers (24–27).

With the aim of following the degradation of Igepal CA 520, we decided to implement the separation of both alkyl and ethoxy chain lengths. This was achieved by using reversed-phase chromatography with a mixture of acetonitrile/water as a mobile phase. As shown in Figure 1, Igepal CA 520 appears as a mixture of three ethoxymers distributions of different alkyl chain (A, B, and C). Analysis of the sample in liquid chromatography/positive electrospray/mass spectrometry allowed us to attribute each peak to a defined APE. It was established that distributions A, B, and C correspond to ethoxymers having a alkyl chain with eight, eight, and four carbons, respectively. The different ranges of the retention times of the mixtures A and B suggest that the APEs of mixture A have alkyl chain structures that are different from those of mixture B. Quantitative analysis of each ethoxymers was performed assuming the independence of the molar extinction coefficient of APE homologues on the number of ethoxy units (28). The area of each peak in the distribution is therefore directly proportional to the concentration of the corresponding APE in solution. Accordingly, we decided in the quantitative studies to neglect the APEs

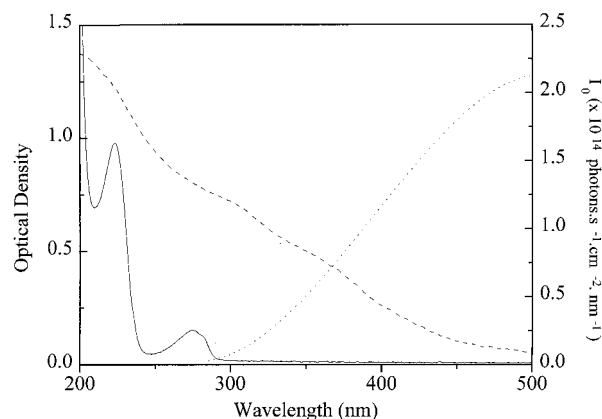


FIGURE 2. UV-vis spectra of (—) aqueous solution of Igepal CA 520 ( $1.0 \times 10^{-4}$  mol L $^{-1}$ ), (---) aqueous solution of Fe(III) [ $3.0 \times 10^{-4}$  mol L $^{-1}$ ; 33% Fe(OH) $^{2+}$ ]; and (···) solar emission in June 1988.

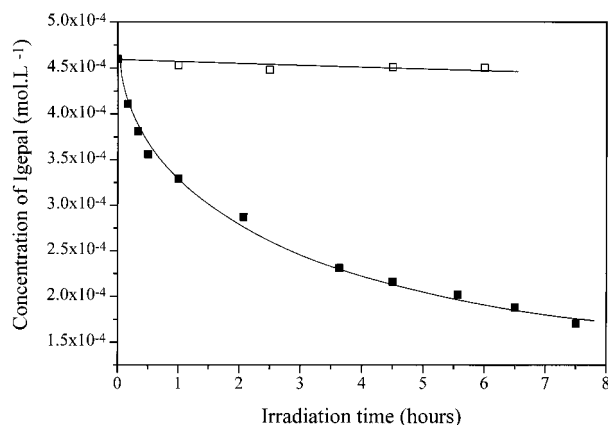


FIGURE 3. Kinetics of Igepal CA 520 disappearance upon irradiation at 365 nm: (□) in the absence of Fe(III), (■) in the presence of Fe(III) [ $3.0 \times 10^{-4}$  mol L $^{-1}$ ; ~100% Fe(OH) $^{2+}$ ].

of the minority distributions B and C, which only represent 1.5% of the total area of the major distribution A.

We also used NMR spectroscopy to obtain information on the structure of the APEs major distribution. The  $^1\text{H}$  NMR spectrum of IGEPAI CA 520 is surprisingly simple: the integration of the proton resonance signals of all the ethylene oxide groups gives  $n = 5$ . This confirms the average degree of ethoxylation  $n = 5$  given for Igepal CA 520. Moreover, the NMR spectrum gives evidence for the presence of a branched alkyl chain.

#### Degradation of Igepal CA 520 Photoinduced by Fe(III).

In this part, Igepal CA 520 refers to the major distribution of ethoxymers A. Igepal CA 520 absorbs in the ultraviolet region with two maxima at 223 nm ( $\epsilon_{\text{max}} = 9400$  L mol $^{-1}$  cm $^{-1}$ ) and 276 nm ( $\epsilon_{\text{max}} = 1300$  L mol $^{-1}$  cm $^{-1}$ ) and with a shoulder at 285 nm. The UV-vis spectrum of the mixture of Igepal/Fe(III) is the sum of the spectra of the two components. There is no detectable complexation in the ground state. Upon irradiation at 365 nm, the light is mainly absorbed by Fe(III) species, the absorption of Igepal CA 520 being very weak at  $\lambda > 300$  nm (Figure 2).  $\cdot\text{OH}$  radicals formed in the photoredox process already described initiate the degradation of Igepal CA 520. Figure 3 compares the disappearance of Igepal CA 520 in the absence and in the presence of Fe(III) [~100% of Fe(OH) $^{2+}$ ]. In the presence of Fe(OH) $^{2+}$ , 60% of a starting Igepal concentration, determined by HPLC, was degraded within 6 h. Upon irradiation the evolution of the area of Igepal CA 520 was the result by two different processes; the disappearance of the starting material and the formation of shorter ethoxymers. In the absence of Fe(III), no significant

degradation took place, indicating that degradation by direct photolysis is negligible.

The disappearance of each ethoxymer of the major distribution was also followed (Figure 4). The rates of disappearance at low conversion percentage ( $\leq 10\%$ ) depend on the concentration of each ethoxymer in the solution. These initial rates were thus corrected for the relative concentration of each ethoxymer.

$$r_{\text{ethoxymer}_n} = \frac{\Delta[E_n]}{\Delta t}$$

$$r_{\text{corrected}} = \frac{\Delta[E_n]}{\Delta t} \frac{[\text{Igepal}]_{\text{total}}}{[E_n]}$$

There is a linear relationship between the so-corrected rates and the number of ethoxy units in the ethoxylated chain (Figure 4, inset). Consequently,  $\cdot\text{OH}$  radicals attack takes place with the same probability whatever the position of the ethoxy unit on the hydrophilic chain. With irradiation time, a dissymmetry appeared in the major distribution: the ethoxymers with high number of ethoxy groups disappeared generating ethoxymers with smaller number of ethoxy units. It was particularly obvious for the ethoxymer with  $n = 1$ , which was in very low concentration in the initial distribution and whose concentration increased in the early stages of the reaction. The shortest compound is octylphenol also detected during the irradiation. These two results reflect the shortening of the ethoxylated chain all along the degradation process.

**Irradiation in the Presence of 2-Propanol.** The degradation of Igepal can be directly attributed to the attack of  $\cdot\text{OH}$  radicals as demonstrated by the 200-fold inhibition of the rate of degradation during irradiation at 365 nm in the presence of 2-propanol (2% v/v), a known  $\cdot\text{OH}$  radical scavenger.

**Influence of the Monomeric Species Concentration.** In this set of experiments, the percentage of Fe(OH) $^{2+}$  species was taken as ~100, 84, 51, and 33%. The initial quantum yields of Igepal disappearance are collected in Table 1. The values of " $\Phi_{\text{Igepal}}$ " are only pseudo values of the quantum yield since the Igepal disappearance is due to a secondary reaction between  $\cdot\text{OH}$  radicals and Igepal. The given value of " $\Phi_{\text{Igepal}}$ " represents the number of molecules disappeared per second divided by the number of photons absorbed by the solution during the same period of time. Table 1 shows that the rate of Igepal disappearance is strongly affected by the Fe(OH) $^{2+}$  percentage: the higher the percentage, the faster the degradation.

**Influence of the Irradiation Wavelength.** To determine the influence of wavelength, solutions of Igepal/Fe(III) ( $1.0 \times 10^{-4}$  mol L $^{-1}$ /  $3.0 \times 10^{-4}$  mol L $^{-1}$ ; ~100% of monomeric species) were monochromatically irradiated at 296, 313, and 365 nm. The initial quantum yields of Igepal disappearance are collected in Table 2. It appears that the rate of Igepal disappearance is also strongly affected by the irradiation wavelength: the lower the wavelength, the faster the degradation. This effect has to be related to the increase of the quantum yield of  $\cdot\text{OH}$  radical formation when the excitation wavelength decreases. It is in agreement with the notion that ejection of  $\cdot\text{OH}$  radical from the solvent cage requires kinetic energy (14).

**Influence of the Igepal CA 520 Concentration.** We investigated the effect of the presence of micelles on the photochemical reaction ( $\text{CMC} = 2.2 \times 10^{-4}$  mol L $^{-1}$ ). Several solutions of Igepal/Fe(III) with initial concentrations of Igepal ranging from  $1.0 \times 10^{-4}$  mol L $^{-1}$  to  $6.0 \times 10^{-4}$  mol L $^{-1}$  were monochromatically irradiated at 365 nm. The initial quantum yields of Igepal disappearance are not affected by the formation of micelles in the solution. We checked the relative

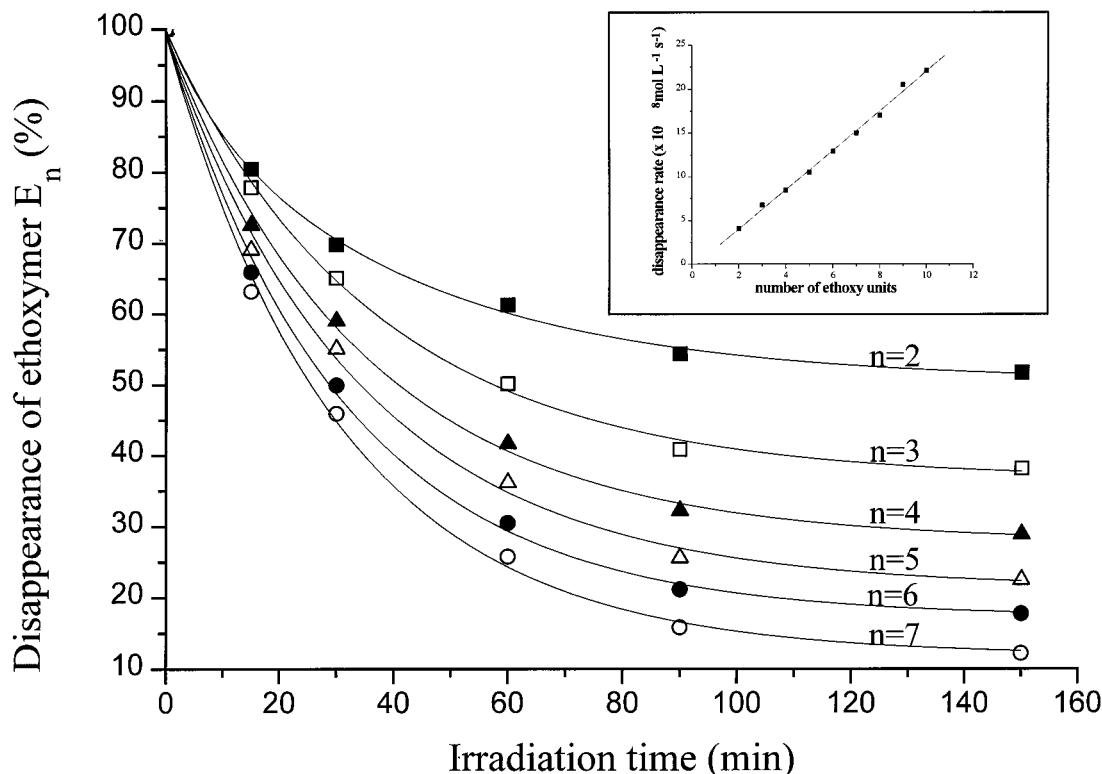


FIGURE 4. Evolution of the percentage of each ethoxymers as a function of irradiation time. Igepal CA 520 ( $4.6 \times 10^{-4} \text{ mol L}^{-1}$ ) and Fe(III) [ $3.0 \times 10^{-4} \text{ mol L}^{-1}$ ;  $\sim 100\% \text{ Fe(OH)}^{2+}$ ]. (Inset) Plot of disappearance rate corrected rates of ethoxymers versus the number of ethoxy units.

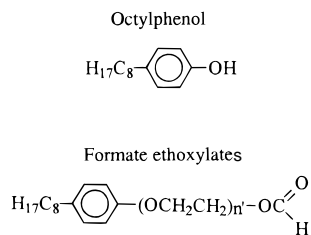
TABLE 1. Influence of the Monomeric Species Concentration on the Initial Quantum Yields of Igepal Disappearance

% of $\text{Fe(OH)}^{2+}$	$\phi$ Igepal
33	0.0018
51	0.0034
84	0.017
$\sim 100$	0.042

concentrations of each ethoxymers in the distribution not to be significantly affected by the total concentration of Igepal, below and above the micellar concentration.

**Photoproduct Identification.** Several peaks appeared in the HPLC chromatogram of an irradiated mixture (Figure 5). The same peaks were observed whatever the percentage of monomeric species or the initial Igepal concentration. Several photoproducts were identified. We noted that the rates of photoproducts formation were strongly affected by the initial  $\text{Fe(OH)}^{2+}$  concentration: they increased with the percentage of  $\text{Fe(OH)}^{2+}$ .

Octylphenol (O) was identified by comparison with the authentic sample.



Formate ethoxylates (F) were identified by mass spectrometry and comparison with authentic samples synthesized in our laboratory. They were obtained by esterification of

TABLE 2. Influence of the Irradiation Wavelength on the Initial Quantum Yields of Igepal Disappearance

irradiation wavelengths (nm)	$\phi$ Igepal
296	0.081
313	0.071
365	0.042

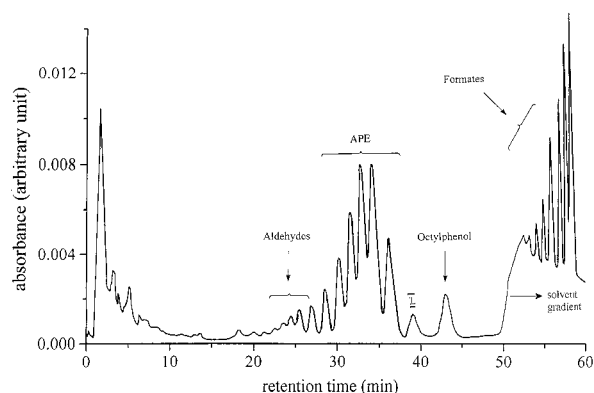


FIGURE 5. HPLC chromatogram of a mixture of Igepal CA 520 ( $4.6 \times 10^{-4} \text{ mol L}^{-1}$ ) and Fe(III) [ $3 \times 10^{-4} \text{ mol L}^{-1}$ ;  $\sim 100\% \text{ Fe(OH)}^{2+}$ ] irradiated 120 min at 365 nm. Detection:  $\lambda = 226 \text{ nm}$ . Eluent: acetonitrile + water (55/45 v/v during 50 min and 80/20 v/v during 10 min).

Igepal CA 520 with formic acid, heating the mixture under reflux for about half an hour in the presence of sulfuric acid. The resulting distribution was roughly symmetrical, whereas formate ethoxylates formed upon irradiation at 365 nm appeared as a disymmetrical distribution as shown in Figure 5. Kinetics of appearance of formates are represented in Figure 6: the lower the degree of ethoxylation, the faster the formation of the corresponding formate. The formate with  $n = 1$  can be formed from any ethoxymers after the attack of

CHART 1

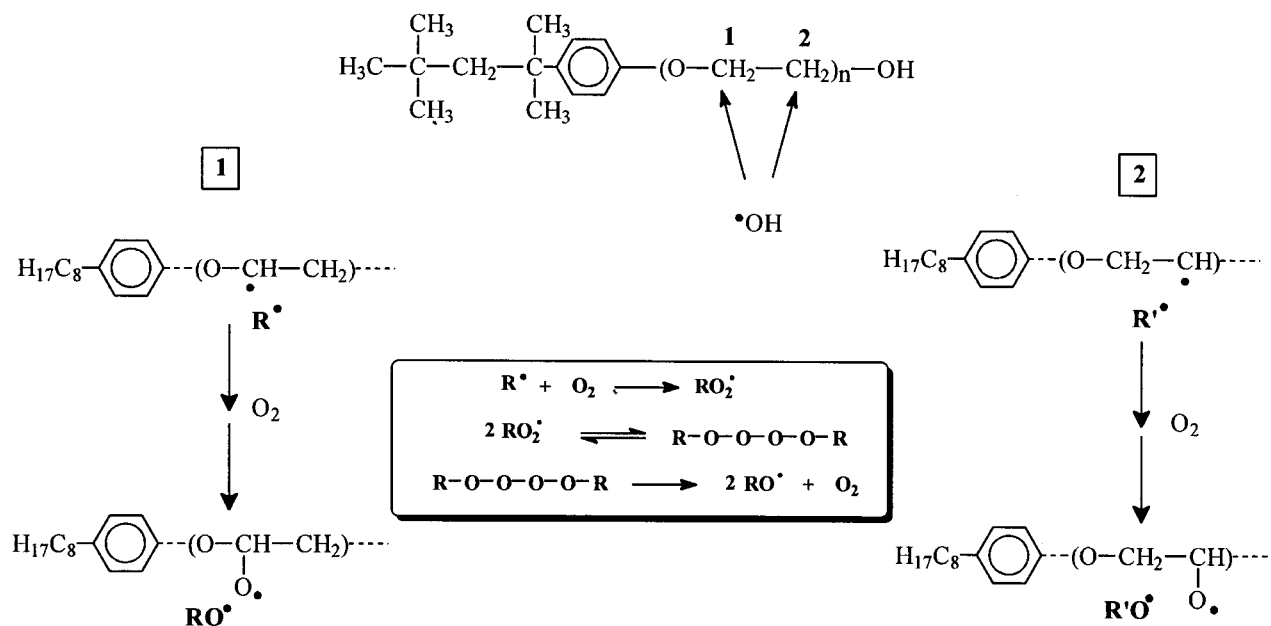
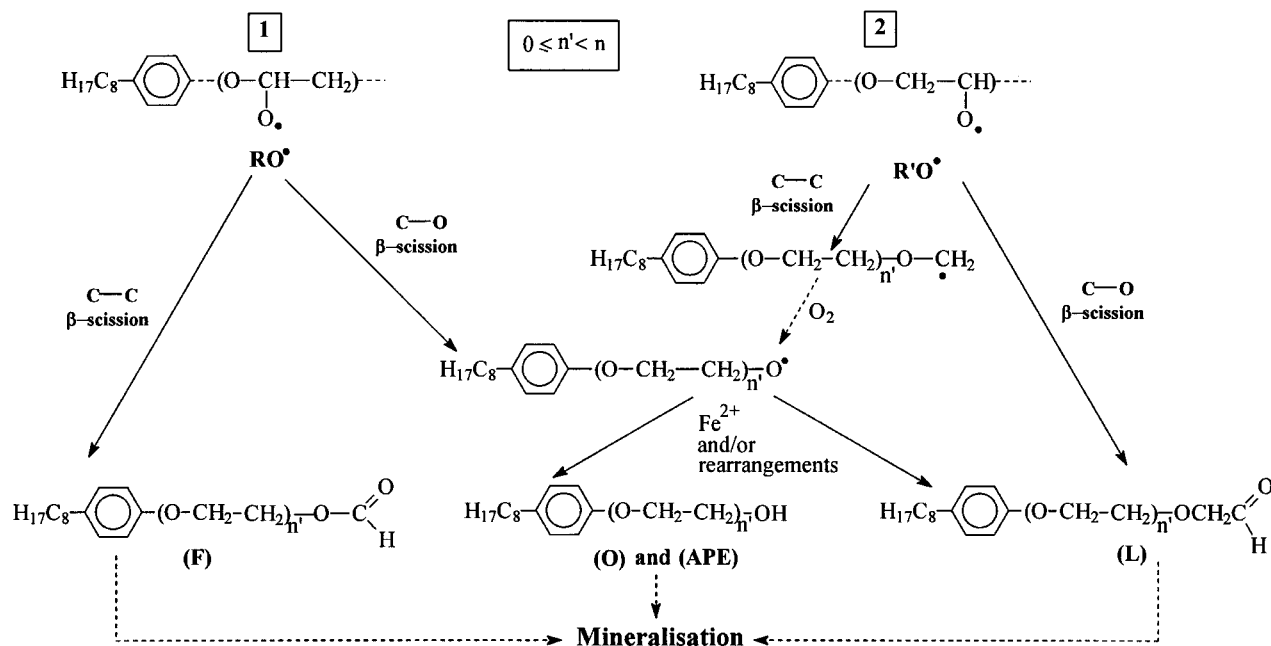


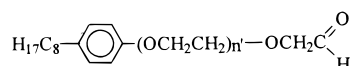
CHART 2



•OH radicals on the first ethoxy group. They are all formed since the beginning of the irradiation.

Aldehyde ethoxylates (L) were identified by mass spectrometry. As they are formed in very low concentrations,

Aldehyde ethoxylates



detailed formation studies were not performed.

The presence of 2-propanol during the irradiation completely prevent the formation of the photoproducts: only traces of formates (F) were detected

**Mechanism of Degradation.** As already mentioned, the first step of the process is the generation of •OH radicals upon irradiation of Fe(III)-aquo complex and more particularly Fe(OH)<sup>2+</sup>. Three different sites can be attacked by

•OH radicals: CH<sub>2</sub> group, and CH<sub>3</sub> groups of the alkyl chain, the aromatic ring, and 2n CH<sub>2</sub> groups of the ethoxylated moiety of the compound. Even though we cannot rule out any attack on the first two sites, the nature of the photo-products gives evidence for a major attack on the poly-ethoxylated chain. In addition, the hydrogen atom of methylene group in α position of either function are far more labile than the hydrogen on the CH<sub>2</sub> group of the alkyl chain. Consequently the attack on the CH<sub>2</sub> groups of the ethoxy chain is highly favored (see Chart 1). The radicals R• and R'•, formed after the abstraction of a hydrogen atom, react with oxygen to form peroxy radicals RO<sub>2</sub>• and R'O<sub>2</sub>•. With peroxy radicals, mono and bimolecular reactions are described (31). In the particular case of the peroxy radical formed from APE, with only one alkoxy group next to the peroxy radical function, the bimolecular reaction is strongly favored: RO<sub>2</sub>• → R-O-O-O-R (32). The decomposition of unstable tetroxides

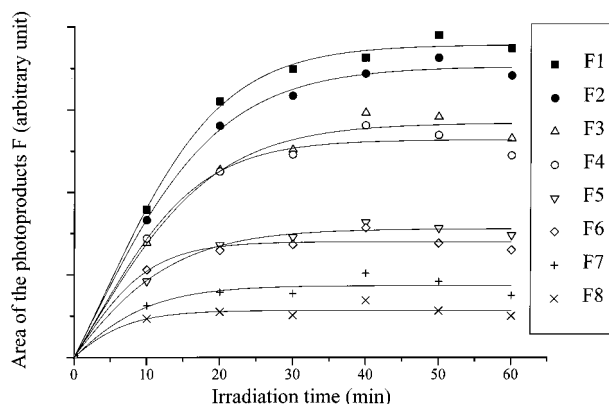


FIGURE 6. Kinetics of formates polyethoxylates appearance during irradiation at 365 nm of a mixture of Igepal CA 520 ( $4.6 \times 10^{-4}$  mol  $L^{-1}$ ) and Fe(III) [ $3.0 \times 10^{-4}$  mol  $L^{-1}$ ;  $\sim 100\%$  Fe(OH) $^{2+}$ ].

into molecular oxygen and two alkoxy radicals is a well-known reaction (31).

Two different routes are then present according to the position of the methylene group attacked by  $\cdot OH$  radicals (see Chart 2).

The attack of  $\cdot OH$  radicals on the first methylene group (1) of an ethoxy unit leads to the alkoxy radical  $RO\cdot$  which undergoes two  $\beta$ -scissions (31): the scission of the C–C bond gives rise to the formate ethoxylates (F); the scission of the C–O bond accounts for the degradation of the Igepal ethoxymers in shorter APEs through an inter or intramolecular rearrangements (31) or a redox reaction with Fe(II). When the initial attack takes place on the first ethoxy unit, this scission gives rise to octylphenol (O).

The attack of  $\cdot OH$  radicals on the second methylene group (2) of an ethoxy unit leads to the alkoxy radical  $R'O\cdot$  which undergoes two  $\beta$ -scissions again; the scission of the C–C bond gives rise to an alkyl radical which undergoes the mechanism already described for this type of radical, and the resulting alkoxy radical leads to the formation of APE with smaller number of ethoxy units; the scission of the C–O bond gives rise to the aldehyde ethoxylates (L).

This mechanism through the formation of an alkoxy radical followed by  $\beta$  scissions allows us to account for all the identified photoproducts.

However, we cannot rule out any formation of the photoproducts either directly from the tetroxide or for some of them by a disproportionation between two alkoxy radicals (31). The formation of the adduct of  $\cdot OH$  radicals with the aromatic ring of APEs is only a very minor importance: any attempt to detect the formation of the resulting hydroxylated photoproducts failed.

**Environmental Significance.** Because our starting motivation was the removal of APEs in water, we tested the efficiency of its degradation photoinduced by Fe(III). This was obtained by following  $CO_2$  evolution during the irradiation ( $\lambda_{irr} = 365$  nm) of an Fe(III)/Igepal solution. The concentrations used for these experiments were  $[Fe(III)] = 3.0 \times 10^{-4}$  mol  $L^{-1}$  and  $[Igepal] = 1.0 \times 10^{-4}$  mol  $L^{-1}$ . The initial monomeric species concentration was near 100%. The  $CO_2$  evolution was calculated with respect to Igepal by considering that Igepal contains an averaged number of 24 atoms of carbon (ethoxymers with  $n = 5$ ) thus yields 24 molecules of  $CO_2$ . Under our experimental conditions, after 3 days of irradiation at 365 nm, 90% of the total mineralization was obtained. A mixture of Igepal CA 520 and Fe(III) was exposed to solar light during a sunny day in September. After 24 h, 90% of the Igepal had disappeared and the photoproducts were similar to those observed under artificial irradiation.

These results are of importance as far as the removal process is concerned: the compounds with an aromatic ring

on either APEs with short alkyl chain or octylphenol, easily detectable by UV detection even at very low concentration, are no longer present in the irradiated solution. The degradation of alkylphenol polyethoxylates in mechanical-biological sewage treatment plants leads to refractory metabolites such as alkylphenol and alkylphenol ethoxylates with one or two oxyethylene groups (4). These compounds are known to be highly toxic to aquatic fauna (33). Even though short APEs or octylphenol are the photoproducts of Igepal degradation photoinduced by Fe(III) in the early stages of the reaction, they are then efficiently degraded by the same process.

## Acknowledgments

The authors indebted to the anonymous reviewers for their helpful comments and suggestions.

## Literature Cited

- Renner, R. *Environ. Sci. Technol.* **1997**, *31*, 316–320.
- Giger, W.; Brunner, P. H.; Schaffner, C. *Science* **1984**, *225*, 623–625.
- Rudling, L.; Solyom, P. *Water Res.* **1974**, *8*, 115–119.
- Stephanou, E.; Giger, W. *Environ. Sci. Technol.* **1982**, *16*, 800–805.
- Ball, H. A.; Reinhard, M.; McCarty, P. L. *Environ. Sci. Technol.* **1989**, *23*, 951–961.
- Fujita, Y.; Reinhard, M. *Environ. Sci. Technol.* **1997**, *31*, 1548–1524.
- Hidaka, H.; Ihara, K.; Fujita, Y.; Yamada, S.; Pelizzetti, E.; Serpone, N. *J. Photochem. Photobiol.* **1988**, *42*, 375–381.
- Pelizzetti, E.; Minero, C.; Maurino, V.; Sclafani, A.; Hidaka, H.; Serpone, N. *Environ. Sci. Technol.* **1989**, *23*, 1380–1385.
- Hidaka, H.; Yamada, S.; Suenaga, S.; Zhao, J.; Serpone, N.; Pelizzetti, E. *J. Mol. Catal.* **1990**, *59*, 279–290.
- Mazellier, P.; Mailhot, G.; Bolte, M. *New J. Chem.* **1997**, *21*, 389–397.
- Mazellier, P.; Jirkovsky, J.; Bolte, M. *Pestic. Sci.* **1997**, *49*, 259–267.
- Brand, N.; Mailhot, G.; Bolte, M. *Chemosphere* **1997**, *34* (12), 2637–2648.
- Faust, B. C.; Hoigné, J. *Atmos. Environ.* **1990**, *24A*, 79–89.
- Benkelberg, H.-J.; Warneck, P. *J. Phys. Chem.* **1995**, *99*, 5214–5221.
- Calvert, J. G.; Pitts, J. M. *Photochemistry*; Wiley: New York, 1966; pp 783–786.
- Küenzi, W. H. *Die Hydrolyse von Eisen (III)*; Ph. D. dissertation ETH no. 7016. Eidgenössischen Technischen Hochschule, Zürich, Switzerland, 1982.
- Longman, G. F. *The analysis of detergents and detergent products*; Wiley: New York, 1975; Vol. 13.
- Cross, J. *Nonionic surfactants: chemical analysis*; Marcel Dekker: New York, 1987.
- Schmitt, T. M. *Analysis of surfactants*; Marcel Dekker: New York, 1992.
- Allen, M. C.; Linder, D. E. *J. Am. Oil Chem. Soc.* **1981**, 950–957.
- Rothman, A. M. *J. Chromatogr.* **1982**, *253*, 283–288.
- Ahel, M.; Giger, W. *Anal. Chem.* **1985**, *57*, 2584–2590.
- Pilc, J. A.; Sermon, P. A. *J. Chromatogr.* **1987**, *398*, 375–380.
- Marcomini, A.; Capri, S.; Giger, W. *J. Chromatogr.* **1987**, *403*, 243–252.
- Schreuder, R. H.; Martijn, A. *J. Chromatogr.* **1988**, *435*, 73–82.
- Marcomini, A.; Filipuzzi, F.; Giger, W. *Chemosphere* **1988**, *17* (5), 853–863.
- Ye, M. Y.; Walkup, R. G.; Hill, K. D. *J. Liq. Chromatogr.* **1995**, *18* (12), 2309–2322.
- Holt, M. S.; McKerrell, E. H.; Perry, J.; Watkinson, R. J. *J. Chromatogr.* **1986**, *362*, 419–424.
- Flynn, C. M. *Chem. Rev.* **1984**, *84* (1), 31–41.
- Knight, R. J.; Sylva, R. N. *J. Inorg. Nucl. Chem.* **1975**, *37*, 779–783.
- Von Sonntag, C.; Schuchmann, H. P. *Angew. Chem., Int. Ed. Engl.* **1991**, *30*, 1229–1253.
- Bennett, J. E.; Howard, J. A. *J. Am. Chem. Soc.* **1973**, *24*, 4008–4010.
- McLeese, D. W.; Zitko, V.; Sergeant, D. B.; Burridge, L.; Metcalfe, C. D. *Chemosphere* **1981**, *10*, 723–734.

Received for review January 15, 1998. Revised manuscript received June 10, 1998. Accepted June 24, 1998.

ES980034V